JOC The Journal of Organic Chemistry

Article

pubs.acs.org/joc

Aromatic C−H Bond Functionalization Induced by Electrochemically in Situ Generated Tris(*p*-bromophenyl)aminium Radical Cation: Cationic Chain Reactions of Electron-Rich Aromatics with Enamides

Long-Ji Li,[†] Yang-Ye Jiang,[†] Chiu Marco Lam,[‡] Cheng-Chu Zeng,*[,†] Li-Ming Hu,[†] and R. Daniel Little*[,‡]

[†]College of Life Science & Bioengineering, Beijing University of Technology, Beijing 100124, China

[‡]Department of Chemistry & Biochemistry, University of California at Santa Barbara, Santa Barbara, California 93106, United States

Supporting Information

ABSTRACT: An effective Friedel−Crafts alkylation reaction of electron-rich aromatics with *N*-vinylamides, induced by electrochemically in situ-generated TBPA radical cation, has been developed; the resulting adducts are produced in good to excellent yields. In the "ex-cell" type electrolysis, TBPA is transformed to its oxidized form in situ and subsequently employed as an electron transfer reagent to initiate a cationic chain reaction. An easily recoverable and reusable polymeric ionic liquid−carbon black (PIL−CB) composite was also utilized as a supporting electrolyte for the electrochemical generation of TBPA cation radical, without sacrificing efficiency or stability after four electrolyses. Cyclic voltammetry analysis and the results of control experiments demonstrate that the reaction of electron-rich aromatics and *N*-vinylamides occurs via a cationic chain reaction, which takes place though an oxidative activation of a C−H bond of electron-rich aromatics instead of oxidation of the *N*-vinylamide as previously assumed.

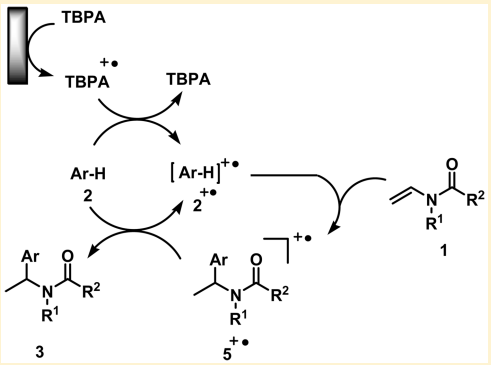

INTRODUCTION

Activation and functionalization of C−H bonds to form new C−C and C−heteroatom bonds has emerged as an important method in organic chemistry because of its step efficiency and atom-economical characteristics.[1] Among existing methods for C−H bond activation and functionalization, a direct oxidative activation using transition metal oxidants or transition metal catalysts in combination with co-oxidants has proven to be one of the most efficient options.[2] However, because toxicity and isolation problems accompany the use of transition metal-based reagents, the development of metal-free, catalytic, oxidative functionalization chemistry is desirable.[3]

Direct electron transfer at an electrode provides an alternative, environmentally benign method for achieving C−H bond functionalization.[4] For example, Yoshida and co-workers have developed an efficient electrochemical C−H oxidative amination method for the synthesis of aromatic primary amines via *N*-arylpyridinium ion intermediates.[4a] On the basis of the same strategy of electrooxidative C−H functionalization, they also achieved direct C−N bond coupling of imidazoles with aromatic and benzylic substrates,[4b] as well as alkene difunctionalization using halogen and chalcogen cation pools stabilized by DMSO.[4c] By utilization of the novel and innovative properties of a boron-doped diamond (BDD) electrode to generate oxyl spin centers, Waldvogel et al. have developed an efficient approach to phenol−arene cross-coupling reactions, forming novel mixed biaryls with high selectivity.[4d−f]

We are interested in oxidative activation and functionalization of C−H bonds via indirect electrolysis, using a redox catalyst that plays the role of the electron transfer agent.[5] In this context, we have explored novel redox catalysts based upon the triarylimidazole scaffold. Among other uses, they have been employed for the oxidative activation of benzylic C−H bonds to afford the corresponding aldehydes, ketones, and benzoates.[6] In addition, we have also applied simple halide ions as redox catalysts to achieve electrochemical C−H bond functionalization, thereby forming new C−N and C−C bonds.[7]

Considering the fact that large amounts of supporting electrolyte are frequently employed in organic electrosynthesis to ensure ionic conductivity and the efficient movement of charge, we have recently developed a PIL−CB composite, which permits an electrolysis to be performed without using a traditional supporting electrolyte, thereby reducing waste and simplifying separation and isolation of the product. One significant advantage of the PIL−CB composite is that it can be efficiently recovered and reused (Scheme 1).[8]

Among well-known organic redox catalysts, tris(*p*-bromophenyl)amine (TBPA) is a versatile and powerful organic redox catalyst and has been widely employed to achieve a variety of processes, including, for example, the deprotection of thioacetals, cleavage of anisyl ethers, oxidation of aromatic side chains, [4+2] cycloaddition reactions,[9] and

Received: September 22, 2015
Published: October 7, 2015

DOI: 10.1021/acs.joc.5b02222
J. Org. Chem. 2015, 80, 11021−11030

Scheme 1. Preparation of the PIL−CB Composite as a Supporting Electrolyte

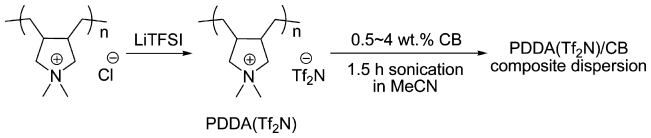

during the key step a total synthesis of a sesquiterpene called daucene.[10] While much effort has been expended, C−H bond functionalization induced by electrochemically in situ-generated TBPA cation radical is limited. In contrast, stable TBPA cation radical salts have been employed to induce C−H bond functionalization. For example, Jia et al. reported the C−H bond functionalization of glycine derivatives to construct a quinolone skeleton with styrene,[11] or 1,4-dihydropyridines with 1,3-dicarbonyl compounds.[12] While stable TBPA cation radical salts such as tris(*p*-bromophenyl)aminium hexachloroantimonate are commercially available, the Lewis acidity of $SbCl_5$, the decomposition product formed upon standing, can render it unsuitable for acid-sensitive substrates unless a hindered base is added as a scavenger.[10,13c] Thus, we chose to form the TBPA cation electrochemically in situ and subsequently use it to promote C−H bond functionalization. This strategy can increase reaction efficiency if the TBPA is recovered by simple chromatographic separation and reused in subsequent reactions.

Herein, we (1) report that the in situ generation of TBPA radical cation does allow the activation of aromatic C−H bonds and induces their Friedel−Crafts alkylation with enamides, (2) demonstrate that a PIL−CB composite can serve as an effective supporting electrolyte in TBPA-mediated chemistry, thus avoiding the employment of a large amount of conducting salt, (3) investigated the mechanism of the coupling process using voltammetry, (4) demonstrate that the homogeneous electron transfer occurs initially between TBPA radical cation and electron-rich aromatics, instead of with an enamide, and (5) determine that the chemistry occurs via a cationic chain reaction pathway. To the best of our knowledge, this work represents the first example using TBPA as a mediator to activate aromatic C−H bonds and induce a cationic chain reaction. We believe that the combination of electrochemically in situ-generated TBPA cation radical and PIL−CB composite as a supporting electrolyte constitutes an attractive electrolytic system for catalytic electrosynthesis.

RESULTS AND DISCUSSION

We commenced our studies by using vinylpyrrolidin-2-one, **1a**, and naphthalene-2-ol, **2a**, as model substrates and performing a controlled potential electrolysis (CPE) at 0.9 V versus Ag/$AgNO_3$, the oxidation peak potential of TBPA, in a divided cell using $LiClO_4/CH_3CN$ as a supporting electrolyte, a platinum net as the working electrode, and an iron plate cathode (Scheme 2 and Table 1). Because monitoring of the reaction

Scheme 2. Electrochemical Alkylation Reaction of Naphthalen-2-ol with Enamide 1a Mediated by TBPA

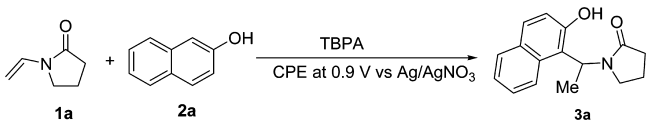

Table 1. Optimization of Reaction Conditions

entry	**2a** (mmol)	**1a** (mmol)	cat. (mol %)	yield (%)
1[a]	0.5	1.0	10	24
2[a]	0.5	1.5	10	50
3[a]	0.5	2.0	10	47
4[b]	0.5	1.5	10	52
5[b]	0.5	1.5	5	37

[a]In-cell. A mixture of substrates **1a**, **2a**, and TBPA was added to the anodic compartment of a divided cell. Controlled potential electrolysis was conducted at 0.9 V vs Ag/$AgNO_3$. [b]Ex-cell. In a divided cell, the $TBPA^{+\bullet}$ was prepared first, the power supply was shut off, and then substrates **1a** and **2a** were added to the anodic compartment at room temperature.

mixture by TLC revealed that vinylpyrrolidinone **1a** was consumed quickly, whereas most of **2a** remained intact, a 2:1 ratio of **1a** to **2a** was subsequently employed. To our delight, the desired adduct **3a** did form, albeit in a 24% isolated yield (Table 1, entry 1). Increasing the amount of **1a** to 3 equiv with respect to **2a** improved the yield of **3a** (Table 1, entry 2). Further increases did not improve the reaction (Table 1, entry 3).

We note that the blue color of the TBPA cation radical is visible while charge is being passed and persists for at least 0.5 h once the current is turned off. This observation, coupled with previous literature, suggested that the reaction of **1a** and **2a** could proceed in a catalytic manner.[13] We envisioned that **3a** might be generated by a so-called "ex-cell" type of indirect electrolysis wherein the TBPA cation radical is first generated in situ and subsequently, in the same (or a separate) cell but without passing additional charge, be used to initiate an electron transfer with the substrates. If it is true, then electrocatalysis should be possible and the amount of current needed to conduct the chemistry should correspond only to that for the oxidation of a substoichiometric quantity of TBPA. Thus, side reactions, resulting from the anodic oxidation of substrates and solvent, as well as overoxidation of products, may be avoided.

To demonstrate this idea, TBPA (10 mol %) was electrolyzed first. After passing 24 C of charge (2.5 F/mol with respect to 0.1 mmol of TBPA), the power supply was turned off and substrates **1a** and **2a** were added to the anodic compartment. After the mixture had been stirred at room temperature for ∼6 h, the desired adduct **3a** could be isolated in a 52% yield (entry 4). In comparison with the in-cell procedure,[5c] the current yield increased, although the yield of **3a** did not improve. Decreasing the amount of TBPA did not improve the outcome. For example, when the amount of TBPA was decreased to 5 mol %, the yield of **3a** decreased to 37%; moreover, more than 10 h was required (Table 1, entry 5). At this stage of our investigation, we concluded that the optimal conditions involved the initial electrochemical generation of 10 mol % $TBPA^{+\bullet}$, followed by treatment of a mixture of electron-rich aromatics and enamide in a molar ratio of 1:3 at room temperature (see Table 1, entry 4).

With the optimal conditions in hand, we turned toward an exploration of the generality and scope of the reaction. As shown in Table 2, the reaction of **1a** and other naphthalene alcohols bearing electron-donating and electron-withdrawing groups proceeded smoothly. For example, when naphthalene-1,7-diol, **1b**, was employed under the standard conditions, the desired product, **3b**, was isolated in an 88% yield, while

DOI: 10.1021/acs.joc.5b02222
J. Org. Chem. 2015, 80, 11021−11030

Table 2. Scope of Electron-Rich Ar−H Partners for the Alkylation Reaction with Vinylpyrrolidin-2-one 1a Mediated by Pre-prepared TBPA$^{+\bullet}$

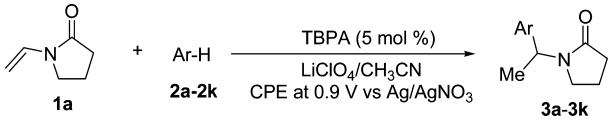

Entry	Ar-H		Product		Yield (%)[a]
1	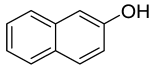	**2a**	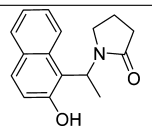	**3a**	52 [b]
2	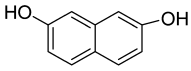	**2b**	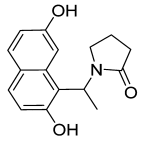	**3b**	88 [b]
3	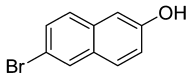	**2c**	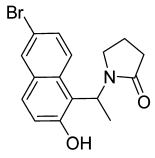	**3c**	30 [b]
4	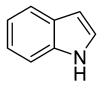	**2d**	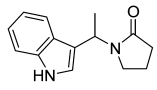	**3d**	93[c]
5	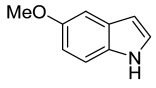	**2e**	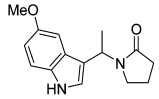	**3e**	85 [c]
6	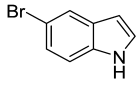	**2f**	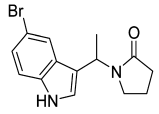	**3f**	91 [c]
7	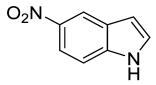	**2g**	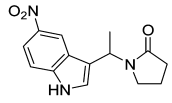	**3g**	60 [c]
8	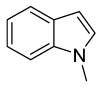	**2h**	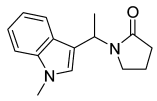	**3h**	86 [c]
9	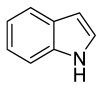	**2d**	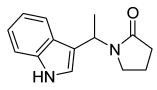	**3d**	93[d]
10		**2i**	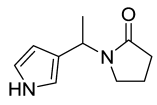	**3i**	63 [c]
11		**2j**	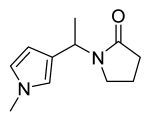	**3j**	69 [c]
12	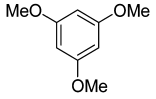	**2k**	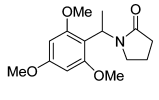	**3k**	70 [c]

[a]Isolated yield following column chromatography. [b]Reaction conditions: TBPA$^{+\bullet}$ (0.1 mmol) was first electrochemically generated in a divided cell containing 10 mL of a $LiClO_4/CH_3CN$ mixture (0.1 mol/L) using a platinum net anode and iron plate cathode and a controlled potential at 0.9 V vs $Ag/AgNO_3$. Subsequently, vinylpyrrolidin-2-one **1a** (3.0 mmol) and arenes **2** (1 mmol) were added, and the mixture was stirred at room temperature. [c]Reaction conditions were similar to those described in footnote *b*, but using vinylpyrrolidin-2-one **1a** (1.0 mmol), arenes **2** (1 mmol), and TBPA (0.05 mmol). [d]Reaction conditions similar to those described in footnote *c*, but using 0.02 mmol of TBPA.

DOI: 10.1021/acs.joc.5b02222
J. Org. Chem. 2015, 80, 11021−11030

Table 3. Scope of Enamide Partners for the Alkylation Reaction Mediated by Pre-prepared TBPA$^{+\bullet}$

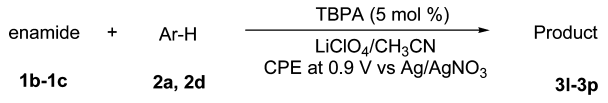

Entry	Enamide		Aromatic	Product		Yield (%)
1[a]	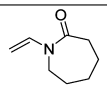	1b	2a	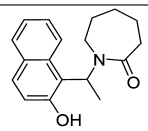	3l	35
2[a]		1c	2a	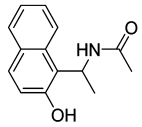	3m	26
3[b]	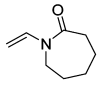	1b	2d	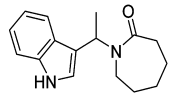	3n	78
4[b]		1c	2d	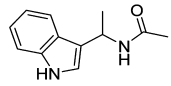	3o	93
5[b]		1c	2d	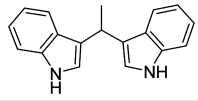	3p	86

[a]Reaction conditions are the same as those described in footnote *b* of Table 2. [b]Reaction conditions are the same as those described in footnote *c* of Table 2.

Table 4. Alkylation Reaction of 2d with 1a in the Presence of the PIL−CB Composite as a Supporting Electrolyte[a]

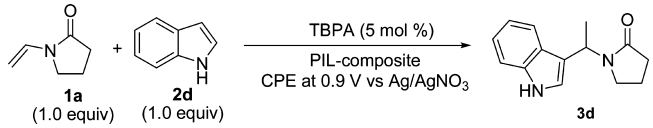

Entry	Product	Yield (%)	Recovery of PIL-composite (%)
1	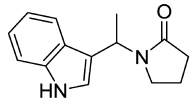 3d	89	98
2		86	97
3		90	97
4		90	98

[a]Reaction conditions: vinylpyrrolidin-2-one **1a** (1.0 mmol), indole **2d** (1 mmol) and TBPA (0.05 mmol) in 10 mL of CH_3CN containing 0.3 M of PDDA(Tf_2N) and 2 wt % of Super P carbon black, divided cell, platinum net anode and iron plate cathode, controlled potential at 0.9 V vs Ag/$AgNO_3$, room temperature.

substrate **1c**, bearing an electron-withdrawing bromide group, gave a slightly lower yield of **3c** (Table 2, entry 3).

Indole derivatives also proved to be suitable candidates. Interestingly, under the standard conditions, the reaction proceeded rapidly and was complete in only 0.5 h, leading to the coupling product and the recovery of excess starting *N*-vinylpyrrolidin-2-one **1a**. In an effort to minimize or entirely avoid the need to recover excess **1a**, further optimization was conducted. When the ratio of **1a** and indole was adjusted to 1:1 and the loading of TBPA reduced to 5 mol %, a 93% isolated yield of coupling product **3d** was achieved in 0.5 h (Table 2, entry 4). Other indole derivatives, bearing electron-donating (MeO) or electron-withdrawing groups (Br and NO_2), also proceeded smoothly to give the corresponding products in good to excellent yields (Table 2, entries 5−7). In the case of *N*-methylindole, adduct **3h** was produced in an 86% yield. Notably, the "ex-cell" electrolysis procedure was so effective that even 2 mol % TBPA led to an excellent yield of **3d**, although a bit longer reaction time (2 vs 0.5 h using 5 mol % TBPA) was needed (Table 2, entry 9). Finally, it was observed that pyrrole, *N*-methylpyrrole, and 1,3,5-trimethoxybenzene were also compatible coupling partners (Table 2, entries 10−12).

To further explore the scope of the chemistry, other *N*-vinylamides were investigated, and the results are summarized in Table 3. It was observed that in contrast with enamide **1a**, the reaction of *N*-vinylamides **1b** and **1c** with naphthalene-2-ol **2a** gave lower yields of coupling products **3l** and **3m** (Table 3, entries 1 and 2). However, the chemistry was more effective in the case of indole. For example, the reaction of 1-vinylazepan-2-one **1b** with indole **2d** gave **3n** in a 78% yield (entry 3). In the case of *N*-vinylacetamide, **1c**, coupling adduct **3o** was obtained

DOI: 10.1021/acs.joc.5b02222
J. Org. Chem. 2015, 80, 11021−11030

in a 93% yield. Notably, a double arylation product **3p** was obtained in excellent yield when 2 equiv of indole was employed to react with **1c**, an outcome that is similar to previous reports.[13a,c] The result is quite significant as structures of this sort are related to the soritins, substances that display unique anti-inflammatory properties.[14]

In the protocol described above, large quantities of $LiClO_4$ were used to render the acetonitrile solution conductive. Of course, the presence of large quantities of an electrolyte leads to separation problems and the production of unwanted waste materials, which detracts from the notion that electroorganic synthesis is a "green and sustainable" process. On the basis of our research involving the use of a polymeric ionic liquid and carbon black composite as a reusable supporting electrolyte,[8] we further investigated the electrocatalytic reaction employing the PIL−CB composite as a surrogate for a traditional supporting electrolyte. As shown in Table 4, the reaction of **1a** with **2d** proceeded smoothly and an 89% yield of **3d** was isolated, nearly the same yield that was obtained using $LiClO_4$ as the supporting electrolyte (note entry 4 of Table 2). Unlike the use of a traditional supporting electrolyte, 98% of the composite was recovered (Table 4, entry 1). To demonstrate the reusability of the PIL−CB composite, the reaction of **1a** and **2d** was repeated four times; each afforded an excellent and stable yield (~90%) and permitted the recovery of >97% of the composite (Table 4, entries 2−4). Furthermore, cyclic voltammograms of the composite before electrolysis and after four electrolyses were nearly the same (Figure 1), thereby revealing that the composite is stable and can survive the electrochemical conditions and further highlighting its utility as a supporting electrolyte surrogate.

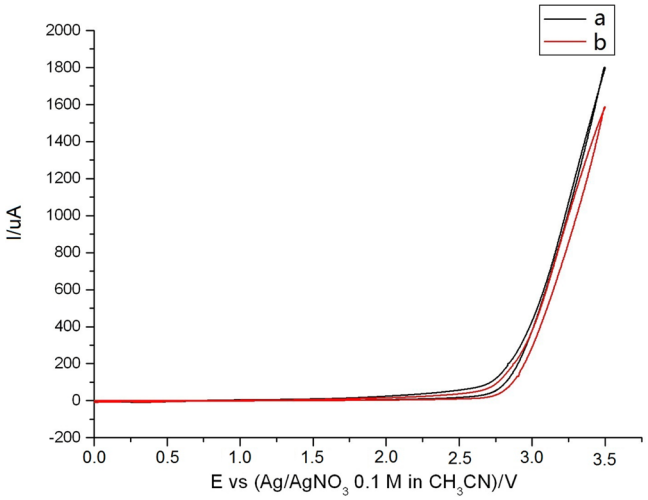

Figure 1. Cyclic voltammogram of the PIL composite (a) before electrolysis and (b) after four electrolyses at a platinum disk working electrode, platinum wire counter, and $Ag/AgNO_3$ (0.1 M in CH_3CN) reference electrodes, in 0.1 M $LiClO_4/CH_3CN$, at a scan rate of 0.1 V/s.

Enamides are widely used as nucleophiles, leading to the introduction of an electrophile at the β-position (Scheme 3a).[15] On the other hand, isomerization of enamides leads to the formation of iminium ion electrophiles, which can then react with a nucleophile (e.g., electron-rich aromatics) and introduce the nucleophile α to the amide nitrogen atom (Scheme 3b).[16] Because Brønsted acids can promote the conversion of

Scheme 3. Two Reaction Pathways of Enamides

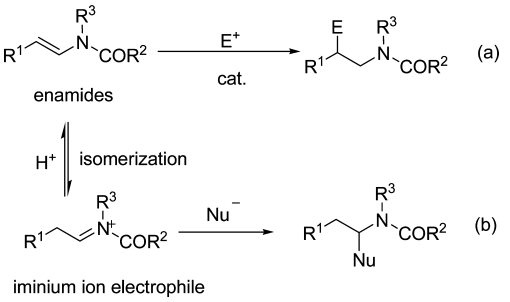

enamides to iminium ion electrophiles,[17] it is reasonable that triarylaminium[13a,e] and Fe(III) salts[13c] have also been utilized to induce Friedel−Crafts arylation of enamides with aromatics, to afford Markovnikov addition products regioselectively.

To investigate the mechanism of the coupling reactions studied in this investigation, we first conducted cyclic voltammetry (CV) analysis of TBPA and related compounds. As shown in Figure 2 and Table 5, TBPA exhibited a well-

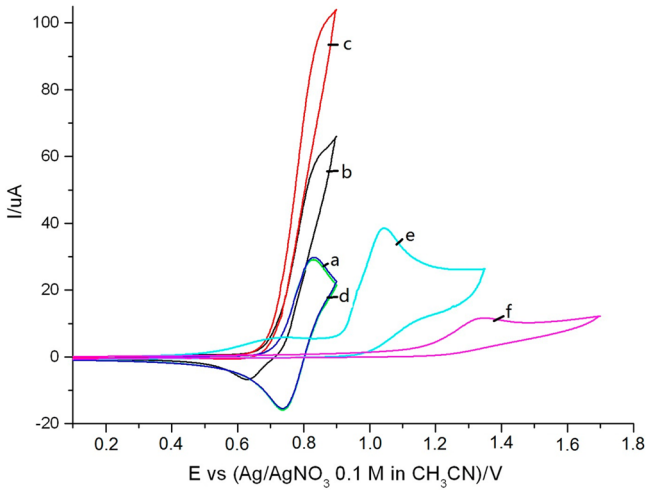

Figure 2. Cyclic voltammograms of TBPA and related compounds in 0.1 M $LiClO_4/CH_3CN$, using a Pt disk working electrode and a Pt wire and $Ag/AgNO_3$ (0.1 M in CH_3CN) as counter and reference electrodes, respectively, at a scan rate of 100 mV/s: (a) TBPA (2 mmol/L), (b) TBPA (2 mmol/L) and naphthalen-2-ol **2a** (5 mmol/L), (c) TBPA (2 mmol/L), naphthalen-2-ol **2a** (5 mmol/L), and *N*-vinylpyrrolin-2-one **1a** (20 mmol/L), (d) TBPA (2 mmol/L) and *N*-vinylpyrrolin-2-one **1a** (10 mmol/L), (e) naphthalen-2-ol **2a** (1 mmol/L), and (f) *N*-vinylpyrrolin-2-one **1a** (1 mol/L).

resolved reversible oxidation wave (peak potential at 0.83 V vs $Ag/AgNO_3$) and reduction wave (peak potential at 0.74 V vs $Ag/AgNO_3$). Voltammograms of all electron-rich aromatics (**2a−k**) and *N*-vinylamides (**1a−c**) were also obtained. Each exhibited one or two irreversible oxidation wave(s) and no cathodic current in the potential scan range of 0.0−2.0 versus $Ag/AgNO_3$ (0.1 M in CH_3CN), a behavior that is typical of a so-called EC process (electrochemical step followed by a chemical step). The results reveal that the electrochemically generated cation radicals of these compounds are not stable on the time scale of the voltammetry measurements and instead engaged in chemical reactions with the solvent or other substrates. As shown in Table 5, the first oxidation potentials, E_{OX}^1, of the electron-rich aromatics (**2a−k**) were lower than

DOI: 10.1021/acs.joc.5b02222
J. Org. Chem. 2015, 80, 11021−11030

Table 5. Peak Potentials of TBPA and Related Compounds[a]

compound	E_{OX}^1 (V)	E_{OX}^2 (V)	compound	E_{OX}^1 (V)	E_{OX}^2 (V)	compound	E_{OX}^1 (V)	E_{OX}^2 (V)
TBPA	0.83	–[b]	**2c**	1.25	–[b]	**2i**	1.30	–[b]
1a	1.34	–[b]	**2d**	0.97	1.40	**2j**	1.13	–[b]
1b	1.33	–[b]	**2e**	0.86	1.23	**2k**	1.32	–[b]
1c	1.58	–[b]	**2f**	1.07	1.29	**3a**	1.05	–[b]
2a	1.04	–[b]	**2g**	1.26	–[b]	**3d**	1.07	–[b]
2b	1.07	–[b]	**2h**	1.02	1.26			

[a]CV conditions: TBPA and related compounds (1 mM) in 0.1 M $LiClO_4/CH_3CN$, platinum disk working electrode, platinum wire counter, and $Ag/AgNO_3$ (0.1 M in CH_3CN) reference electrode. Scan rate of 0.1 V/s. [b]There is only one oxidation peak in the range of 0.0–2.0 vs $Ag/AgNO_3$.

Scheme 4. Control Experiments

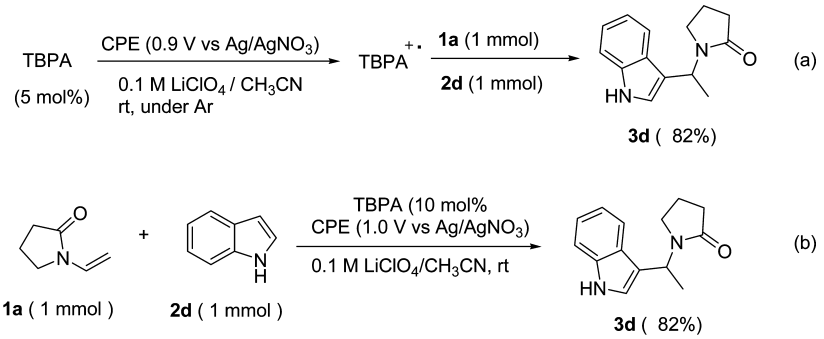

Table 6. Natural and Mulliken Atomic Charges for 1a and Its Cation Radical

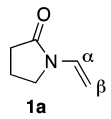

1a

atom	neutral (**1a**) [a]		cation radical (**1a**$^{+\bullet}$) [a]	
alpha (α)	– 0.019	– 0.010	0.055	0.007
beta (β)	– 0.518	– 0.451	– 0.209	– 0.264
	natural	Mulliken	natural	Mulliken

[a]Atomic charges (both "natural" and "Mulliken"); values obtained from B3LYP/6-31+G(d) calculations.

those of the *N*-vinylamides (**1a–c**), implying that the initial electron transfer will preferentially occur between $TBPA^{+\bullet}$ and the aromatics rather than the enamides.

The electrochemical behavior of TBPA in the presence of *N*-vinylpyrrolin-2-one, **1a**, and naphthalen-2-ol, **2a**, further demonstrates that the electrochemically generated TBPA cation radical undergoes electron transfer with **2a**. As shown in Figure 2 (curve b), a dramatic enhancement of the anodic current of TBPA (24 μA vs 55 μA) was observed and was accompanied by a decrease in the cathodic current when 2.5 equiv of naphthalen-2-ol **2a** was added to the solution of TBPA in CH_3CN. Because the oxidation peak potential of **2a** appears at 1.04 V versus $Ag/AgNO_3$, a value that is greater than that of TBPA (0.83 V vs $Ag/AgNO_3$), the increase in the anodic peak current corresponds to a catalytic current that reflects turnover of the TBPA–$TBPA^{+\bullet}$ redox couple.[5c] The observation indicates that the homogeneous electron transfer process between $TPBA^{\bullet+}$ and naphthalen-2-ol **2a** occurs rapidly.

When both *N*-vinylpyrrolin-2-one **1a** (10 equiv) and **2a** were added to the TBPA solution, the anodic current increased once again, this time from 55 to 87 μA (compare curves a–c). We suggest that the additional increase likely involves the formation of the cation radical of **2a**, thereby increasing the acidity of the OH proton, followed by a protonation at the β-carbon of the vinylamide and subsequent capture. On the other hand, comparison of curves a and d reveals that the voltammogram for TBPA when recorded in the presence of *N*-vinylpyrrolin-2-one **1a** alone is nearly identical to that recorded for TBPA in its absence. This outcome indicates that a direct electron transfer between *N*-vinylpyrrolin-2-one **1a** and $TBPA^{+\bullet}$ does not occur. That TBPA does not serve as an efficient redox catalyst for the anodic oxidation of **1a** is reasonable when one compares the peak potentials of TBPA and **1a** (curve f), the difference being sufficiently large (>0.6 V) to establish an insurmountable thermodynamic impasse. On the basis of the results described above, we conclude that the initial electron transfer occurs between $TBPA^{+\bullet}$ and the aromatics rather than the enamide substrates.

To gain additional insight into the reaction mechanism, a series of control experiments were performed. As shown in Scheme 4a, TBPA (5 mol %) was initially oxidized at its peak potential (0.9 V vs $Ag/AgNO_3$) to form its cation radical; subsequently, **1a** (1 mmol) and indole **2d** (1 mmol) were added to conduct the alkylation reaction under an argon atmosphere. After routine workup, **3d** was isolated in an 82% yield. The result rules out the possibility that oxygen regenerates $TBPA^{+\bullet}$ and supports the idea that the reaction is a $TBPA^{+\bullet}$-induced chain process.

Controlled potential electrolysis of the mixture of **1a** and indole, **2d**, in the presence of TBPA, conducted at the peak potential of indole (1.0 V vs $Ag/AgNO_3$), also gave **3d** in 82% yield (Scheme 4b). By virtue of the fact that **1a** (E_{OX}^1 = 1.34 V vs $Ag/AgNO_3$) is more difficult to oxidize than **2d** (E_{OX}^1 = 0.97 V vs $Ag/AgNO_3$) and that CPE was conducted at 1.0 V versus $Ag/AgNO_3$, it is consequently safe to conclude that it is the electron-rich aromatic **2d**, instead of **1a**, that initially undergoes

DOI: 10.1021/acs.joc.5b02222
J. Org. Chem. 2015, 80, 11021–11030

electrochemical oxidation to form its cation radical, and subsequently reacting with **1a** to generate final product **3d**.

In addition, examination of the products reveals that coupling occurs between a nucleophilic center of the aromatic and the α-carbon of the enamide, implying that the α-carbon serves as an electrophilic site. To account for this outcome, we recall that while voltammetry establishes that an iminium ion is not formed initially, the conversion of enamides to iminium ion electrophiles could possibly be promoted by the initial cation radical $\mathbf{2}^{+\bullet}$, which will discussed later. To gain additional insight, we calculated the atomic charges at both the α- and β-carbons of the neutral and cation radical forms of *N*-vinylpyrrolin-2-one (**1a** and $\mathbf{1a}^{+\bullet}$, respectively) using the B3LYP method and a diffuse 6-31+G(d) basis set. The results, displayed in Table 6, list both the natural and Mulliken atomic charges, each simply representing an alternative method for calculating charge. The fact that the largest charge resides on the β-carbon in the neutral form, **1a**, is entirely consistent with its nucleophilic character. The cation radical is more interesting. Here, the atomic charge at the β-carbon is diminished relative to that of the neutral form (−0.518) but remains substantial (−0.209). The α-carbon on the other hand becomes a hole, with an atomic charge of +0.055 (natural, and +0.007 Mulliken). Thus, the α-carbon of the cation radical becomes an attractive location for attack by a nucleophilic aromatic coupling partner, in accord with the experimental outcome.

On the basis of the CV analysis and the control experiments described above, we propose that the reaction of electron-rich aromatics with *N*-vinylamides mediated by electrochemically in situ-generated TBPA cation radical involves a cationic chain reaction pathway. Quite different from chemically preprepared triarylaminium salt- and Fe(III) salt-induced chain reaction of enamides and aromatics, in which isomerization of enamides to form iminium ion electrophiles is the first step,[13] our electrochemical chain reaction starts with the formation of cation radical $\mathbf{2}^{+\bullet}$ generated via a homogeneous electron transfer between electron-rich aromatics **2** and $\text{TBPA}^{+\bullet}$, which is generated electrochemically in situ.

The formation of cation radical $\mathbf{2}^{+\bullet}$ increases the acidity of the O−H (for naphthols **2a**−**c**) or N−H (for N-unsubstituted indoles, **2d**−**f**, or pyrrole, **2i**) bond, which leads to a protonation of the *N*-vinylamide (Scheme 5). In the cases of **2h**, **2j**, and **2k**, their corresponding cation radicals ($\mathbf{2h}^{+\bullet}$, $\mathbf{2j}^{+\bullet}$, and $\mathbf{2k}^{+\bullet}$, respectively), formed from homogeneous electron transfer with $\text{TBPA}^{+\bullet}$, serve as Lewis acids. Both types of cation radical $\mathbf{2}^{+\bullet}$ promote the conversion of the *N*-vinylamide to an iminium ion electrophile. Once formed, the electron deficient α-carbon is subsequently attacked by the electron-rich aromatic to afford a new cation radical, $\mathbf{4}^{+\bullet}$. From there, a second homogeneous electron transfer between **2** and $\mathbf{4}^{+\bullet}$ produces coupling product **3** and regenerates $\mathbf{2}^{+\bullet}$. The regeneration of $\mathbf{2}^{+\bullet}$ allows the chain propagation to proceed. In this manner, the electrochemical initiation (viz., the first electron transfer between $\text{TBPA}^{+\bullet}$ and Ar−H) is excluded from the subsequent chain reaction processes. Because only a catalytic amount of charge is required to generate a substoichiometric amount of $\text{TBPA}^{+\bullet}$, ≫100% current yields are achieved.

Scheme 5. A Plausible Mechanism for the Cationic Chain Reaction

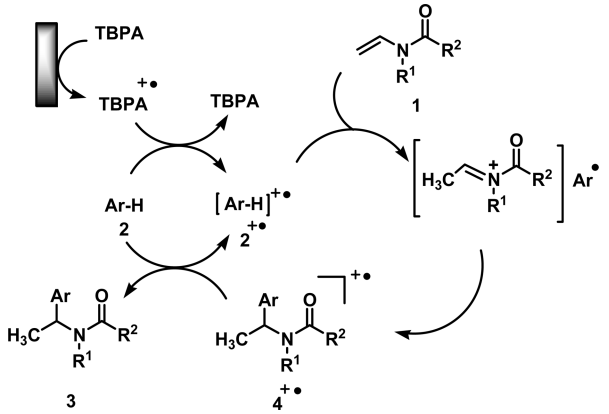

CONCLUSIONS

In summary, an effective electrochemical protocol for the Friedel−Crafts alkylation of electron-rich aromatics with *N*-vinylamides has been developed, and the corresponding adducts form in good to excellent yields. In the protocol, the TBPA cation radical is generated electrochemically in situ and subsequently employed as an electron transfer regent to initiate a cationic chain reaction. The reusable PIL−CB composite developed by us previously could be utilized as a supporting electrolyte for the electrochemical generation of TBPA cation radical, without sacrificing efficiency, and remained stable after four electrolyses. Cyclic voltammetry analysis and control experiments demonstrate that the reaction of *N*-vinylamides with electron-rich aromatics occurs through a cationic chain reaction mechanism, via initial oxidative activation of the electron-rich aromatics, instead of oxidation of the *N*-vinylamide as previously assumed. The results further demonstrate the versatility of TBPA as a redox mediator in indirect electrolysis. In addition, the combination of electrochemically in situ-generated TBPA cation radical and a PIL composite as a supporting electrolyte has proven to be an attractive electrolytic system for catalytic electrosynthesis. Their application to other types of reactions is underway in our laboratory.

EXPERIMENTAL SECTION

Instruments and Reagents. All melting points were measured with an Electrothermal melting point apparatus and are uncorrected. IR spectra were recorded using KBr pellets. NMR spectra were recorded with a 400 MHz spectrometer (400 MHz ^{1}H frequency, 100 MHz ^{13}C frequency). Chemical shifts are given as δ values (internal standard, TMS). Coupling constants are reported in hertz. High resolution mass spectral data was obtained using the electrospray ionization method and an ion trap mass analyzer. Other chemicals and solvents were obtained from a commercial resource and used without further purification.

Cyclic Voltammetry. Cyclic voltammograms were measured using a Princeton Applied Research 273A potentiostat/galvanostat equipped with electrochemical analysis software, using a conventional three-electrode cell. The working electrode was a glassy carbon disk electrode (ϕ ∼ 3 mm). The auxiliary and reference electrodes consisted of a Pt wire and $Ag/AgNO_3$ (0.1 M in CH_3CN), respectively. Glassy carbon was polished with a polishing cloth before each measurement. All electrodes for CV experiments were obtained from CH Instruments, Inc. The concentration of all tested compounds was 1 mmol L^{-1}, while that of the supporting electrolyte was 0.1 mol L^{-1}.

General Procedures for In-Cell Electrolysis. An H type cell equipped with a 4G porosity glass frit to separate the anode and cathode compartments was used. A platinum mesh (2 cm × 3 cm) served as the working electrode; an Fe plate served as the counter

DOI: 10.1021/acs.joc.5b02222
J. Org. Chem. 2015, 80, 11021−11030

electrode, and a $Ag/AgNO_3$ (0.1 M) electrode was used as the reference electrode. The solution of 0.1 M $LiClO_4/CH_3CN$ was added to the two compartments (10 mL × 2), each equipped with a magnetic stir bar. Then the substrate **1a** (1.5 mmol), **2a** (0.5 mmol), and the mediator, TBPA (10 or 5 mol %), were added to the anodic compartment. After connection to the constant-voltage power supply, the electrolysis was performed at a potential of 0.9 V (vs $Ag/AgNO_3$) and terminated when TLC analysis showed that the starting **1a** had been consumed. Then the solvent was removed under reduced pressure, and extraction was conducted using CH_2Cl_2 (3 × 15 mL). The combined organic layers were washed with a saturated aqueous NaCl solution and dried over $MgSO_4$. The purified product was obtained after column chromatography on silica gel using a solvent mixture of petroleum ether and ethyl acetate.

General Procedures for Ex-Cell Electrolysis. An H type cell equipped with a 4G porosity glass frit to separate the anode and cathode compartments was used. A platinum mesh (2 cm × 3 cm) served as the working electrode; an Fe plate served as the counter electrode, and a $Ag/AgNO_3$ (0.1 M) electrode was used as the reference electrode. The 0.1 M $LiClO_4/CH_3CN$ solution was added to the two compartments (10 mL × 2), each equipped with a magnetic stir bar. Then the mediator, TBPA, was added to the working electrode compartment. The solutions were degassed with argon for 10 min before the electrolysis, and an argon atmosphere was maintained throughout. At 0 °C, electrolysis was performed at a potential of 0.9 V (vs $Ag/AgNO_3$) and terminated when 2.5 F/mol (12 C) of charge had been consumed.

The electrodes were then removed, and substrates **1** and **2** were quickly added to the anodic compartment. Under ambient conditions, the resulting solution was stirred until the TLC analysis showed that starting material **1** had been consumed. Then the solvent was removed under reduced pressure, and extraction was conducted using CH_2Cl_2 (3 × 15 mL). The combined organic layers were washed with a saturated aqueous NaCl solution and dried over $MgSO_4$. The purified product was obtained after column chromatography on silica gel using a solvent mixture of petroleum ether and ethyl acetate.

General Procedures for Ex-Cell Type Electrolysis Using the Composite as the Supporting Electrolyte. An H type cell equipped with a 4G porosity glass frit to separate the anode and cathode compartments was used. A platinum mesh (2 cm × 3 cm) served as the working electrode; an Fe plate served as the counter electrode, and a $Ag/AgNO_3$ (0.1 M) electrode was used as the reference electrode. The preprepared PDDA(Tf_2N)/CB composite dispersion[8] was added in equal volumes to the anode and cathode compartments of the H type cell that was equipped with a magnetic stir bar in each compartment. Then the mediator, TBPA, was added to the anodic compartment. The solutions were degassed with argon for 10 min before the electrolysis, and an argon atmosphere was maintained throughout. Electrolysis was performed at 0 °C at a potential of 0.9 V (vs $Ag/AgNO_3$) and terminated when 2.5 F/mol (12 C) of charge had been consumed.

The electrodes were then removed, and substrates **1** and **2** were quickly added to the anodic compartment. Under ambient conditions, the reaction mixture was stirred until the TLC analysis showed that the starting **1** had been consumed. Then the solvent was removed under reduced pressure; extraction was conducted using CH_2Cl_2 (3 × 15 mL), and an extended period of stirring in DCM was conducted to maximize the separation and isolation of the crude product from the composite. The crude reaction mixture was rinsed with additional DCM; the combined DCM solutions were washed with water and brine, and the organic layer was dried over $MgSO_4$. The purified product was obtained after column chromatography on silica gel using a solvent mixture of petroleum ether and ethyl acetate.

Recovery of the Composite. Following vacuum filtration, the composite was collected, dried in a vacuum oven at 80 °C, and weighed periodically. Drying was continued until the mass of the composite remained constant.

Regeneration of the Composite Dispersion. The recovered composite was once again converted into a stable dispersion via the addition of acetonitrile and, if needed, sonication using a simple laboratory sonicator.

Reuse of the Composite Dispersion. The regenerated composite dispersion was added to the H type cell as the electrolyte, and electrolysis was conducted as described above.

1-[1-(2-Hydroxynaphthalen-1-yl)ethyl]pyrrolidin-2-one (3a).[13a] Isolated as a white solid (67 mg, 0.26 mmol, 52% yield): ^{1}H NMR (400 MHz, $CDCl_3$) δ 1.97 (d, J = 7.6 Hz, 3H), 2.04−2.10 (m, 2H), 2.45−2.50 (m, 2H), 3.67−3.73 (m, 1H), 3.81−3.87 (m, 1H), 5.72 (q, J = 7.2 Hz, 1H), 7.23 (d, J = 9.2 Hz, 1H), 7.33 (t, J = 7.4 Hz, 1H), 7.47−7.51 (m, 1H), 7.72 (d, J = 8.8 Hz, 1H), 7.79 (d, J = 8.0 Hz, 1H), 8.05 (d, J = 8.8 Hz, 1H), 10.14 (s, 1H); ^{13}C NMR (100 MHz, $CDCl_3$) δ 16.8, 18.3, 31.5, 47.5, 48.6, 118.1, 121.5, 122.2, 122.7, 126.5, 129.2, 129.4, 130.2, 133.1, 154.9, 177.2.

1-[1-(2,7-Dihydroxynaphthalen-1-yl)ethyl]pyrrolidin-2-one (3b).[13a] Isolated as a white solid (119 mg, 0.43 mmol, 88% yield): ^{1}H NMR (400 MHz, DMSO-d_6) δ 1.65 (d, J = 6.8 Hz, 3H), 1.72−1.93 (m, 2H), 2.13−2.29 (m, 2H), 3.14−3.20 (m, 1H), 3.55−3.60 (m, 1H), 5.76 (q, J = 7.2 Hz, 1H), 6.84 (d, J = 8.4 Hz, 1H), 6.90 (d, J = 8.8 Hz, 1H), 7.32 (s, 1H), 7.54 (d, J = 8.8 Hz, 1H), 7.58 (d, J = 8.8 Hz, 1H), 9.56 (s, 1H), 9.65 (s, 1H); ^{13}C NMR (100 MHz, DMSO-d_6) δ 17.8, 18.0, 31.2, 44.4, 45.2, 105.3, 115.2, 115.6, 116.1, 123.5, 129.5, 130.4, 135.6, 155.3, 156.5, 173.6.

1-[1-(6-Bromo-2-hydroxynaphthalen-1-yl)ethyl]pyrrolidin-2-one (3c).[13a] Isolated as a white solid (50 mg, 0.15 mmol, 30% yield): ^{1}H NMR (400 MHz, DMSO-d_6) δ 1.76 (d, J = 7.2 Hz, 3H), 1.78−1.90 (m, 2H), 2.08−2.50 (m, 2H), 3.14−3.20 (m, 1H), 3.54−3.60 (m, 1H), 5.88 (q, J = 7.2 Hz, 1H), 7.20 (d, J = 8.8 Hz, 1H), 7.53 (d, J = 9.2 Hz, 1H), 7.72 (d, J = 9.2 Hz, 1H), 8.04 (s, 1H), 8.07 (d, J = 9.2 Hz, 1H), 10.02 (s, 1H); ^{13}C NMR (100 MHz, DMSO-d_6) δ 22.4, 22.8, 35.8, 48.9, 49.7, 120.5, 122.4, 125.6, 130.3, 133.7, 134.4, 134.8, 135.3, 137.2, 160.2, 178.3.

1-[1-(1*H*-Indol-3-yl)ethyl]pyrrolidin-2-one (3d).[18] Isolated as a white solid (212 mg, 0.93 mmol, 93% yield): ^{1}H NMR (400 MHz, $CDCl_3$) δ 1.61 (d, J = 6.8 Hz, 3H), 1.79−1.84 (m, 1H), 1.90−1.95 (m, 1H), 2.44−2.49 (m, 2H), 2.86−2.92 (m, 1H), 3.26−3.32 (m, 1H), 5.81 (q, J = 6.8 Hz, 1H), 7.11 (t, J = 7.2 Hz, 1H), 7.15 (s, 1H), 7.23 (t, J = 8.0 Hz, 1H), 7.39 (d, J = 8.0 Hz, 1H), 7.65 (d, J = 7.6 Hz, 1H), 8.38 (s, 1H); ^{13}C NMR (100 MHz, $CDCl_3$) δ 16.7, 17.8, 31.8, 42.3, 42.7, 111.3, 115.8, 119.4, 119.8, 122.3, 122.3, 126.5, 136.6, 174.4.

1-[1-(5-Methoxy-1*H*-indol-3-yl)ethyl]pyrrolidin-2-one (3e).[18] Isolated as a white solid (219 mg, 0.85 mmol, 85% yield, at room temperature): ^{1}H NMR (400 MHz, $CDCl_3$) δ 1.57 (d, J = 7.2 Hz, 3H), 1.74−1.94 (m, 2H), 2.39−2.50 (m, 2H), 2.84−2.87 (m, 1H), 3.24−3.27 (m, 1H), 3.79 (s, 3H), 5.78 (q, J = 6.8 Hz, 1H), 6.84 (dd, J = 8.8 Hz, 2.4 Hz, 1H), 7.10−7.13 (m, 2H), 7.25−7.27 (d, J = 8.8 Hz, 1H), 9.48 (s, 1H); ^{13}C NMR (100 MHz, $CDCl_3$) δ 16.7, 17.7, 31.9, 42.3, 42.8, 55.8, 100.7, 112.2, 112.5, 115.1, 123.2, 126.8, 131.8, 154.0, 174.6.

1-[1-(5-Bromo-1*H*-indol-3-yl)ethyl]pyrrolidin-2-one (3f).[18] Isolated as a white solid (278 mg, 0.91 mmol, 91% yield, at room temperature): ^{1}H NMR (400 MHz, $CDCl_3$) δ 1.58 (d, J = 6.4 Hz, 3H), 1.79−1.96 (m, 2H), 2.47 (t, J = 8.2 Hz, 2H), 2.84−2.89 (m, 1H), 3.25−3.31 (m, 1H), 5.71 (q, J = 6.8 Hz, 1H), 7.16 (d, J = 2.0 Hz, 1H), 7.27−7.28 (m, 2H), 7.73 (s, 1H), 9.03 (s, 1H); ^{13}C NMR (100 MHz, $CDCl_3$) δ 16.7, 17.8, 31.7, 42.3, 42.6, 112.7, 113.2, 115.8, 121.9, 123.4, 125.4, 128.1, 135.2, 174.4.

1-[1-(5-Nitro-1*H*-indol-3-yl)ethyl]pyrrolidin-2-one (3g).[18] Isolated as a yellow solid (164 mg, 0.60 mmol, 60% yield, at room temperature): ^{1}H NMR (400 MHz, DMSO-d_6) δ 1.54 (d, J = 6.8 Hz, 3H), 1.70−1.86 (m, 2H), 2.21−2.31 (m, 2H), 2.72−2.75 (m, 1H), 3.27−3.32 (m, 1H), 5.59 (q, J = 6.8 Hz, 1H), 7.53 (d, J = 8.8 Hz, 1H), 7.64 (s, 1H), 7.80 (dd, J = 8.8, 2.0 Hz, 1H), 8.45 (d, J = 1.6 Hz, 1H), 11.79 (s, 1H); ^{13}C NMR (100 MHz, DMSO-d_6) δ 21.9, 22.5, 36.2, 46.5, 46.6, 117.2, 121.0, 122.1, 122.8, 130.6, 132.4, 144.8, 145.8, 178.4.

1-[1-(1-Methyl-1*H*-indol-3-yl)ethyl]pyrrolidin-2-one (3h).[18] Isolated as a yellow oil (208 mg, 0.86 mmol, 86% yield, at room temperature): ^{1}H NMR (400 MHz, $CDCl_3$) δ 1.60 (d, J = 6.8 Hz, 3H), 1.77−1.95 (m, 2H), 2.40−2.49 (m, 2H), 2.88−2.94 (m, 1H), 3.26−3.32 (m, 1H), 3.78 (s, 3H), 5.79 (q, J = 6.8 Hz, 1H), 6.99 (s,

DOI: 10.1021/acs.joc.5b02222
J. Org. Chem. 2015, 80, 11021−11030

1H), 7.11 (t, J = 8.0 Hz, 1H), 7.25 (t, J = 7.2 Hz, 1H), 7.31 (d, J = 8.0 Hz, 1H), 7.63 (d, J = 8.0 Hz, 1H); ^{13}C NMR (100 MHz, $CDCl_3$) δ 16.8, 17.8, 31.8, 32.8, 42.2, 42.6, 109.2, 114.6, 119.5, 119.7, 122.1, 126.7, 126.9, 137.2, 174.2.

1-[1-(1*H*-Pyrrol-2-yl)ethyl]pyrrolidin-2-one (3i).[13d] Isolated as a gray solid (112 mg, 0.63 mmol, 63% yield, at room temperature): ^{1}H NMR (400 MHz, $CDCl_3$) δ 1.55 (d, J = 7.2 Hz, 3H), 1.92−2.04 (m, 2H), 2.34−2.50 (m, 2H), 3.09−3.15 (m, 1H), 3.36−3.42 (m, 1H), 5.35 (q, J = 7.2 Hz, 1H), 6.10−6.12 (m, 2H), 6.74 (s, 1H); ^{13}C NMR (100 MHz, $CDCl_3$) δ 15.9, 17.7, 31.6, 42.6, 44.1, 105.4, 107.3, 118.1, 131.8, 175.5.

1-[1-(1-Methyl-1*H*-pyrrol-2-yl)ethyl]pyrrolidin-2-one (3j). Isolated as a colorless oil (132.5 mg, 0.69 mmol, 69% yield): ^{1}H NMR (400 MHz, $CDCl_3$) δ 1.51 (d, J = 7.2 Hz, 3H), 1.87−1.99 (m, 2H), 2.35−2.49 (m, 2H), 2.83−2.89 (m, 1H), 3.26−3.32 (m, 1H), 3.52 (s, 3H), 5.46 (q, J = 6.8 Hz, 2H), 6.06−6.08 (m, 1H), 6.14−6.15 (m, 1H), 6.61 (t, J = 2.0 Hz, 1H); ^{13}C NMR (100 MHz, $CDCl_3$) δ 16.6, 17.8, 31.6, 33.8, 42.2, 42.2, 106.5, 107.4, 122.8, 131.1, 173.8; IR (KBr) 2977, 1681, 1494, 1420, 1285, 1208, 716 cm^{-1}; HRMS (ESI positive) calcd for $C_{11}H_{16}N_2O$ $[M + H]^+$ 193.1341, found 193.1332.

1-[1-(2,4,6-Trimethoxyphenyl)ethyl]pyrrolidin-2-one (3k).[5] Isolated as a white solid (195 mg, 0.70 mmol, 70% yield): ^{1}H NMR (400 MHz, $CDCl_3$) δ 1.50 (d, J = 7.6 Hz, 3H), 1.80−1.98 (m, 2H), 2.26−2.39 (m, 2H), 3.23−3.28 (m, 1H), 3.51−3.58 (m, 1H), 3.81 (s, 9H), 5.85 (q, J = 7.2 Hz, 1H), 6.12 (s, 2H); ^{13}C NMR (100 MHz, $CDCl_3$) δ 17.2, 18.2, 31.5, 42.5, 44.4, 55.3, 55.7, 91.0, 109.7, 159.9, 160.4, 174.0.

1-[1-(2-Hydroxynaphthalen-1-yl)ethyl]azepan-2-one (3l).[13a] Isolated as a white solid (49.5 mg, 0.17 mmol, 35% yield): ^{1}H NMR (400 MHz, $CDCl_3$) δ 1.55−1.73 (m, 6H), 1.92 (d, J = 7.2 Hz, 3H), 2.60−2.65 (m, 2H), 3.58−3.60 (m, 2H), 5.75 (q, J = 7.2 Hz, 1H), 7.18 (d, J = 8.8 Hz, 1H), 7.32 (t, J = 7.6 Hz, 1H), 7.49 (t, J = 7.6 Hz, 1H), 7.71 (d, J = 8.8 Hz, 1H), 7.79 (d, J = 8.0 Hz, 1H), 7.98 (d, J = 8.8 Hz, 1H), 9.91 (s, 1H); ^{13}C NMR (100 MHz, DMSO-d_6) δ 19.0, 23.4, 28.7, 29.4, 37.1, 43.9, 48.41, 116.3, 119.8, 123.1, 123.2, 127.1, 128.9, 130.0, 134.6, 155.6, 173.2.

***N*-[1-(2-Hydroxynaphthalen-1-yl)ethyl]acetamide (3m).**[13a] Isolated as a white solid (30 mg, 0.27 mmol, 26% yield): ^{1}H NMR (400 MHz, DMSO-d_6) δ 1.50 (d, J = 8.8 Hz, 1H), 1.82 (s, 3H), 5.85 (q, J = 7.2 Hz, 1H), 7.16 (d, J = 8.8 Hz, 1H), 7.26−7.29 (m, 1H), 7.43−7.47 (m, 2H), 7.67 (d, J = 8.8 Hz, 1H), 7.78 (d, J = 8.0 Hz, 1H), 8.10 (d, J = 8.8 Hz, 1H), 8.13 (s, 1H), 9.88 (s, 1H); ^{13}C NMR (100 MHz, DMSO-d_6) δ 20.6, 23.2, 42.1, 119.1, 121.0, 122.7, 123.0, 126.6, 128.8, 128.8, 129.0, 132.3, 153.2, 168.7.

1-[1-(1*H*-Indol-3-yl)ethyl]azepan-2-one (3n).[18] Isolated as a white solid (200 mg, 0.78 mmol, 78% yield): ^{1}H NMR (400 MHz, $CDCl_3$) δ 1.16−1.30 (m, 3H), 1.53 (d, J = 6.8 Hz, 3H), 1.67−1.71 (m, 3H), 2.62−2.64 (m, 2H), 3.02−3.19 (m, 2H), 6.33 (q, J = 6.8 Hz, 1H), 7.12 (t, J = 7.6 Hz, 1H), 7.15 (d, J = 1.2 Hz, 1H), 7.20 (t, J = 7.4 Hz, 1H), 7.38 (d, J = 8.0 Hz, 1H), 7.62 (d, J = 7.6 Hz, 1H), 8.45 (s, 1H); ^{13}C NMR (100 MHz, $CDCl_3$) δ 17.1, 23.5, 29.0, 30.1, 37.9, 42.9, 45.1, 111.2, 116.7, 119.7, 119.8, 122.3, 122.6, 126.7, 136.6, 175.6.

***N*-[1-(1*H*-Indol-3-yl)ethyl]acetamide (3o).**[18] Isolated as a white solid (188 mg, 0.93 mmol, 93% yield): ^{1}H NMR (400 MHz, $CDCl_3$) δ 1.65 (d, J = 6.4 Hz, 3H), 1.99 (s, 3H), 5.46−5.52 (m, 1H), 5.74−5.75 (m, 1H), 7.13−7.14 (m, 2H), 7.24 (t, J = 7.6 Hz, 1H), 7.40 (d, J = 8.4 Hz, 1H), 7.68 (d, J = 8.0 Hz, 1H), 8.41 (s, 1H); ^{13}C NMR (100 MHz, $CDCl_3$) δ 14.3, 20.6, 21.1, 23.4, 42.1, 60.6, 111.7, 115.7, 117.5, 119.2, 119.5, 121.8, 122.2, 126.0, 129.6, 136.8, 169.8.

3,3′-(Ethane-1,1-diyl)bis(1*H*-indole) (3p).[13b] Isolated as a white solid (223 mg, 0.86 mmol, 86% yield): ^{1}H NMR (400 MHz, $CDCl_3$) δ 1.85 (d, J = 7.2 Hz, 3H), 4.72 (q, J = 7.2 Hz, 1H), 6.91 (d, J = 1.6 Hz, 2H), 7.08−7.12 (m, 2H), 7.20−7.24 (m, 2H), 7.36 (d, J = 8.0 Hz, 2H), 7.63 (d, J = 8.0 Hz, 2H), 7.81 (s, 1H); ^{13}C NMR (100 MHz, $CDCl_3$) δ 21.8, 28.2, 111.2, 119.1, 119.8, 121.3, 121.7, 121.8, 126.9, 136.7.

■ ASSOCIATED CONTENT

Supporting Information

The Supporting Information is available free of charge on the ACS Publications website at DOI: 10.1021/acs.joc.5b02222.

Copies of ^{1}H and ^{13}C NMR spectra of all compounds and HRMS spectra of new compound **3j** (PDF)

■ AUTHOR INFORMATION

Corresponding Authors

*E-mail: zengcc@bjut.edu.cn. Fax: 86-10-67396211. Telephone: 86-10-67396211.

*E-mail: little@ucsb.chem.edu. Fax: 805-893-4120. Telephone: 805-893-3693.

Notes

The authors declare no competing financial interest.

■ ACKNOWLEDGMENTS

This work was supported by grants from the National Natural Science Foundation of China (21272021 and 21472011) and the National Key Technology R&D Program (2011BAD23B01). C.-C.Z. and R.D.L. are grateful to the U.S. National Science Foundation-supported PIRE-ECCI program (OISE-0968399) and the Center for the Sustainable Use of Renewable Feedstocks (CenSURF), a National Science Foundation Center for Chemical Innovation (CHE-1240194), for fostering our international collaboration.

■ REFERENCES

(1) For recent reviews, see: (a) Yu, J. Q., Shi, Z. J., Eds. *Topics in Current Chemistry: C−H activation*; Springer: Berlin, 2010; Vol. 292. (b) Yeung, C. S.; Dong, V. M. *Chem. Rev.* **2011**, *111*, 1215−1292. (c) Cho, S. H.; Kim, J. Y.; Kwak, J.; Chang, S. *Chem. Soc. Rev.* **2011**, *40*, 5068−5083. (d) Ackermann, L. *Chem. Rev.* **2011**, *111*, 1315−1345. (e) Xu, L. M.; Li, B. J.; Yang, Z.; Shi, Z. J. *Chem. Soc. Rev.* **2010**, *39*, 712−733. (f) Louillat, M. L.; Patureau, F. W. *Chem. Soc. Rev.* **2014**, *43*, 901−910.

(2) For selected examples, see: (a) Tsang, W. C. P.; Zheng, N.; Buchwald, S. L. *J. Am. Chem. Soc.* **2005**, *127*, 14560−14561. (b) Wang, H.; Wang, Y.; Peng, C.; Zhang, J.; Zhu, Q. *J. Am. Chem. Soc.* **2010**, *132*, 13217−13219. (c) Wang, X.; Jin, Y.; Zhao, Y.; Zhu, L.; Fu, F. *Org. Lett.* **2012**, *14*, 5030−5033. (d) Armstrong, A.; Collins, J. C. *Angew. Chem., Int. Ed.* **2010**, *49*, 2282−2285. (e) Xiao, B.; Gong, T. J.; Xu, J.; Liu, Z. J.; Liu, L. *J. Am. Chem. Soc.* **2011**, *133*, 1466−1474. (f) Shrestha, R.; Mukherjee, P.; Tan, Y.; Litman, Z. C.; Hartwig, J. F. *J. Am. Chem. Soc.* **2013**, *135*, 8480−8483.

(3) For excellent reviews on metal-free oxidative C−H functionalization, see: (a) Sun, C. L.; Li, B.-J.; Shi, Z.-J. *Chem. Rev.* **2011**, *111*, 1293−1314. (b) Samanta, R.; Matcha, K.; Antonchick, A. P. *Eur. J. Org. Chem.* **2013**, *2013*, 5769−5804.

(4) (a) Morofuji, T.; Shimizu, A.; Yoshida, J. I. *J. Am. Chem. Soc.* **2013**, *135*, 5000−5003. (b) Morofuji, T.; Shimizu, A.; Yoshida, J. I. *J. Am. Chem. Soc.* **2014**, *136*, 4496−4499. (c) Ashikari, Y.; Shimizu, A.; Nokami, T.; Yoshida, J. I. *J. Am. Chem. Soc.* **2013**, *135*, 16070−16073. (d) Elsler, B.; Schollmeyer, D.; Dyballa, K. M.; Franke, R.; Waldvogel, S. R. *Angew. Chem., Int. Ed.* **2014**, *53*, 5210−5213. (e) Kirste, A.; Schnakenburg, G.; Stecker, F.; Fischer, A.; Waldvogel, S. R. *Angew. Chem., Int. Ed.* **2010**, *49*, 971−975. (f) Kirste, A.; Elsler, B.; Schnakenburg, G.; Waldvogel, S. R. *J. Am. Chem. Soc.* **2012**, *134*, 3571−3576.

(5) For reviews of indirect electrolysis, see: (a) Francke, R.; Little, R. D. *Chem. Soc. Rev.* **2014**, *43*, 2492−2521. (b) Ogibin, Y. N.; Elinson, M. N.; Nikishin, G. I. *Russ. Chem. Rev.* **2009**, *78*, 89−140. (c) Steckhan, E. *Angew. Chem., Int. Ed. Engl.* **1986**, *25*, 683−701.

(6) (a) Zeng, C. C.; Zhang, N. T.; Lam, M.; Little, R. D. *Org. Lett.* **2012**, *14*, 1314−1317. (b) Zhang, N. T.; Zeng, C. C.; Lam, C. M.;

DOI: 10.1021/acs.joc.5b02222
J. Org. Chem. 2015, 80, 11021−11030

Gbur, R. K.; Little, R. D. *J. Org. Chem.* **2013**, *78*, 2104−2110. (c) Lu, N. N.; Zhang, N. T.; Zeng, C. C.; Hu, L. M.; Yoo, S. J.; Little, R. D. *J. Org. Chem.* **2015**, *80*, 781−789. (d) Lu, N. N.; Yoo, S. J.; Li, L. J.; Zeng, C. C.; Little, R. D. *Electrochim. Acta* **2014**, *142*, 254−260.

(7) (a) Chen, J.; Yan, W. Q.; Lam, C. M.; Zeng, C. C.; Hu, L. M.; Little, R. D. *Org. Lett.* **2015**, *17*, 986−989. (b) Gao, W. J.; Li, W. C.; Zeng, C. C.; Tian, H. Y.; Hu, L. M.; Little, R. D. *J. Org. Chem.* **2014**, *79*, 9613−9618. (c) Li, W. C.; Zeng, C. C.; Hu, L. M.; Tian, H. Y.; Little, R. D. *Adv. Synth. Catal.* **2013**, *355*, 2884−2890. (d) Li, W. C.; Zhang, Z. Z.; Zeng, C. C.; Hu, L. M.; Tian, H. Y. *Curr. Org. Synth.* **2014**, *11*, 454−460.

(8) Yoo, S. J.; Li, L. J.; Zeng, C. C.; Little, R. D. *Angew. Chem., Int. Ed.* **2015**, *54*, 3744−3747.

(9) (a) Steckhan, E. *Top. Curr. Chem.* **1987**, *142*, 1−69 and references cited therein. (b) Steckhan, E. *Angew. Chem., Int. Ed. Engl.* **1986**, *25*, 683−701 and references cited therein. For recent excellent examples, see: (c) Shen, Y.; Hattori, H.; Ding, K.; Atobe, M.; Fuchigami, T. *Electrochim. Acta* **2006**, *51*, 2819−2824. (d) Wu, X.; Davis, A. P.; Fry, A. J. *Org. Lett.* **2007**, *9*, 5633−5636.

(10) Park, Y. S.; Little, R. D. *J. Org. Chem.* **2008**, *73*, 6807−6815.

(11) (a) Liu, J.; Liu, F.; Zhu, Y. Z.; Ma, X. G.; Jia, X. D. *Org. Lett.* **2015**, *17*, 1409−1412. (b) Wang, Y. X.; Peng, F. F.; Liu, J.; Huo, C.; Wang, X. C.; Jia, X. D. *J. Org. Chem.* **2015**, *80*, 609−614. (c) Jia, X. D.; Peng, F. F.; Qing, C.; Huo, C.; Wang, X. C. *Org. Lett.* **2012**, *14*, 4030−4033. (d) Jia, X. D.; Wang, Y. X.; Peng, F. F.; Huo, C.; Yu, L. L.; Liu, J.; Wang, X. C. *J. Org. Chem.* **2013**, *78*, 9450−9456.

(12) (a) Jia, X. D.; Wang, Y. X.; Peng, F. F.; Huo, C.; Yu, L. L.; Liu, J.; Wang, X. C. *Adv. Synth. Catal.* **2014**, *356*, 1210−1216. (b) Liu, J.; Wang, Y. X.; Yu, L. L.; Huo, C.; Wang, X. C.; Jia, X. D. *Adv. Synth. Catal.* **2014**, *356*, 3214−3218.

(13) (a) Huo, C.; Kang, L. S.; Xu, X. L.; Jia, X. D.; Wang, X. C.; Yuan, Y.; Xie, H. *Tetrahedron* **2014**, *70*, 1055−1059. (b) Jiang, R.; Xu, H. Y.; Xu, X. P.; Chu, X. Q.; Ji, S. J. *Org. Biomol. Chem.* **2011**, *9*, 5659−5669. (c) Niu, T. M.; Huang, L. H.; Wu, T. X.; Zhang, Y. H. *Org. Biomol. Chem.* **2011**, *9*, 273−277. (d) Jiang, R.; Wu, X. J.; Zhu, X.; Xu, X. P.; Ji, S. J. *Eur. J. Org. Chem.* **2010**, *2010*, 5946−5950. (e) Huo, C.; Kang, L. S.; Xu, X. L.; Jia, X. D.; Wang, X. C.; Xie, H. S.; Yuan, Y. *Tetrahedron Lett.* **2014**, *55*, 954−958.

(14) (a) Jacobs, R. S.; Little, R. D. Method for the Synthesis of Soritin Compounds. U.S. Patent 7,074,938 B2, 2004. (b) Mattern, R.; Wright, A. E.; Jacobs, R. S. Bis-indole Derivatives and Their Use as Antiinflammatory Agents. CA Patent 2,335,254 A1, 2000.

(15) (a) Carbery, D. R. *Org. Biomol. Chem.* **2008**, *6*, 3455−3460. (b) Matsubara, R.; Kobayashi, S. *Acc. Chem. Res.* **2008**, *41*, 292−301.

(16) (a) Terada, M.; Sorimachi, K. *J. Am. Chem. Soc.* **2007**, *129*, 292−293. (b) Jia, Y. X.; Zhong, J.; Zhu, S. F.; Zhang, C. M.; Zhou, Q. L. *Angew. Chem., Int. Ed.* **2007**, *46*, 5565−5567.

(17) (a) Yang, L.; Zheng, Q. Y.; Wang, D. X.; Huang, Z. T.; Wang, M. X. *Org. Lett.* **2008**, *10*, 2461−2464. (b) Zu, L.; Xie, H.; Li, H.; Wang, J.; Yu, X.; Wang, W. *Chem. - Eur. J.* **2008**, *14*, 6333−6335. (c) Dagousset, G.; Drouet, F.; Masson, G.; Zhu, J. *Org. Lett.* **2009**, *11*, 5546−5549.

(18) Huo, C.; Kang, L.; Xu, X.; Jia, X.; Wang, X.; Xie, H.; Yuan, Y. *Tetrahedron Lett.* **2014**, *55*, 264−266.

DOI: 10.1021/acs.joc.5b02222
J. Org. Chem. 2015, 80, 11021−11030